OPTOELECTRONICS AND ADVANCED MATERIALS – RAPID COMMUNICATIONS Vol. 1, No. 11, November 2007, p. 583 - 587

2d numerical modeling and simulation of a non-uniform doped electric field dependent MESFET photodetector

M. KABEER[a], V. RAJAMANI[*]
Department of Electronics and Communication Engineering, P.S.N.A. College of Engineering and Technology, Dindigul – 624 622, Tamil Nadu, India
[a]Department of Information Technology, B.S. Abdur Rahman Crescent Engg. College, Chennai, Tamilnadu, India

Numerical simulation of a non-uniform doped optically gated GaAs MESFET photodetector for the characterization of the device as photodetector has been presented in this paper. The model involves the solution of a 2D Poissons equation with proper boundary conditions and the field dependent mobility of the cariers in the channels for the computation of the drain current. It has been found that in a short channel MESFET photodetector, the drain current saturation is caused by the velocity saturation of the carriers rather than the pinch off condition. The non uniform doping density in the channel, the electric filed along the x and y direction has also been calculated numerically. We have also computed the transimpendence and the drain resistance of the GaAs MESFET numerically. It has been seen that the two dimensional modeling provides better accurate solution and closely fit with the experimental results. The model can be used as basic tool for an accurate simulation of MESFET photodetector for the OEIC applications.

(Received September 3, 2007; accepted October 31, 2007)

Keywords: 2D numerical modeling, GaAs MESFET photodetector, Non-uniform doping profile, Field dependent photocurrent

1. Introduction

The transmission of billions bits of information per second through a single optical fiber over long distance is possible through the optical communication technology. As optical components continue to replace electronic component for high speed optical signal processing applications, there is a growing impetus to put more optical devices onto a single chip. The full exploitation of the information carrying capacity of the optical fibers needs the development of optical sources and detectors capable of handling data rates at such high rates [1-3]. The GaAs MESFETs can be used as a photodetector due to its higher carrier mobility and its potentiality. The optically controlled MESFET was named as Optical Field Effect Transistor (OPFET) and was introduced as a novel high speed optical detector by Gammel et al [5]. The light induced voltage and the current characteristics of an optically controlled microwave device were reported analytically by Simons et al [2]. The switching characteristics of GaAs MESFET considering modulated illumination up to microwave ranges has been reported by Paolella et al [3]. It was concluded that the GaAs MESFET has higher sensitivity than InP MESFET. The microwave circuit parameters of the GaAs MESFETs in the linear and saturation regions were experimentally reported by Gautier et al [4]. The response speed of 50 to 100 ps with the photo conductive gain of 2 to 5 can be achieved with OPFET. The photo induced voltages at the schottky contact (V_{op}) as well as at the junction between channel and substrate (V_{ops}) are calculated for one dimensional GaAs MESFET by Madheswaran et al [7]. GaAs MESFETs, are useful for low noise amplification, high efficiency and high speed logic amplification. The absence of parasitics in GaAs MESFETs produces faster response time. A Complete characterization of the devices requires the numerical modeling. In this paper, we present a two dimensional numerical simulation of GaAs MESFET with non uniform doped profile in the channel. The potential distribution through the channel has also been calculated under both dark and illuminated conditions.

2. Modeling of GaAs MESFET photo detector

The model has been developed considering the channel is non-uniformly doped. Modeling has been done to calculate various parameters such as carrier concentration, potential distributions, depletion layer thickness, electric field mobility, drain characteristics and trans-conductance. The two-dimensional (2-D) Poisson's equation in the gate-depletion region in the illuminated condition with the Schottky contact as the reference can be written as,

$$\nabla^2\psi(x,y)=\frac{-q}{\varepsilon_s}\left[N_d(x,y)-\frac{P_{opt}(1-R_m)(1-R_s)\alpha\tau_L e^{-\alpha y}}{h\nu}+\frac{r_s}{S}\right] \quad (1)$$

where $\psi(x,y)$ the 2-D potential distribution, ε_s is the permittivity of the GaAs, R_m and R_s are the reflection coefficient at the entrance and at the metal semiconductor contact respectively, P_{opt} is the incident optical power density, h is the Planck's constant, ν is the frequency of the incident radiation, α is the optical absorption

coefficient of the semiconductor at the operating wavelength, r_s is the surface recombination rate, S is the surface recombination velocity, τ_L is the mean lifetime of the minority carriers under illumination and q is the electron charge.

N_d (x,y) is the non uniform doping density and its value has been calculated by solving two dimensional Gaussian's distribution function given by

$$N_d(x,y)=\frac{Q}{(2\Pi)^{3/2}\Delta R_p \Delta R^2_T}\exp-\left(\frac{x}{\sqrt{2\Delta R^2_T}}\right)^2 \exp-\left(\frac{Y-R_p}{\sqrt{2\Delta R^2_p}}\right)^2 \quad (2)$$

where, ΔR_p is the projected straggle, ΔR_T is the transverse straggle, R_p is the projected rangte, Q is the number of implanted ions. The depletion widths at the source and drain is given by

$$y_S = \left[2\xi_s \frac{(V_G + V_{bi})}{qN_d(x,y)}\right]^{1/2} \quad (3)$$

$$y_d = \left[2\xi_s \frac{(V_G + V_D + V_{bi})}{qN_d(x,y)}\right]^{1/2} \quad (4)$$

The boundary conditions to solve the 2D Poisson's equations are,

$$\begin{aligned} \psi(x,y)\big|_{y=0} &= V_{gs} - \phi_{bi} \\ \psi(x,y)\big|_{x=0} &= V_{bi} + V_{OP} \\ \psi(x,y)\big|_{x=L} &= V_{bi} + V_{OP} + V_{ds} \\ \psi(x,y)\big|_{y=tsi} &= \psi_{bp}(x) \end{aligned} \quad (5)$$

where V_{gs} is the gate to source voltage, V_{ds} is the drain to source voltage, Φ_{bi} is the built-in voltage of the schottky barrier gate, $\psi_{bp}(x)$ is the bottom potential for non-uniform doping profile, V_{bi} is the built in voltage between the channel to the source junction and V_{OP} is the photo induced voltage.

The excess carriers generated in the semiconductor due to the absorption of incident optical power is given by

$$\Delta n = \frac{\sqrt{1+\frac{4\tau P_{opt}(1-R_m)(1-R_s)(1-e^{-\alpha W_m})}{W_m h\gamma n_i}}-1}{\frac{2P_{opt}(1-R_m)(1-R_s)(1-e^{-\alpha W_m})}{W_m h\gamma n_i}} \quad (6)$$

where W_m is the maximum width of the depletion layer, R_m, R_i, R_s are the reflection coefficient at the metal gate entrance, gate-insulator interface and the insulator-semiconductor interface respectively. The width of the depletion layer is written as

$$W_m = \left[4\varepsilon_s \ln\left(\frac{P_{po}}{n_i}\right)\Big/ q\beta P_{p0}\right]^{1/2} \quad (7)$$

In order to obtain the surface potential as a function of x and y, equation (1) has been solved using the boundary conditions. The potential at the surface end of the gate is the sum of built-in voltage and applied drain voltage. The mean lifetime of the minority carriers in the illuminated condition, τ_1 can be written as

$$\tau_1 = \left(\frac{n_i}{n_i + \Delta n}\right)\tau \quad (8)$$

The characteristics of the device in the absence of illumination can be obtained in a similar way by substituting $P_{opt} = 0$ in appropriate equations.

The basic model equation (1) has been solved numerically using Liebmann's iteration method. The channel profile has been obtained by dividing the channel region into several meshes and the potential distributions have been obtained using the appropriate boundary condition. The length of the channel is divided into equal meshes 'mx' in longitudinal direction and 'my' in the transversal direction and hence equation (1) has been rewritten as follows

$$\psi_{ij}(x,y)=\sum_{i=0}^{\frac{L}{mx}}\sum_{j=0}^{\frac{y_{dg}}{my}}\left\{\begin{aligned}&\psi(i-1,j)+\psi(i+1,j)+\psi(i,j-1)+\psi(i,j+1)\\&+\frac{q}{\varepsilon_s}\left[N_d(x,y)-\frac{P_{opt}(1-R_m)(1-R_s)\alpha\tau_L e^{-\alpha y}}{h\nu}+\frac{r_s}{S}\right]\end{aligned}\right\} \quad (9)$$

The electric fields along the x and y direction have been obtained from the two dimensional potential distribution in the channel by solving equations

$$E_x = \frac{\psi(i+1,j)-\psi(i-1,j)}{2L/mx} \quad (10)$$

$$E_y = \frac{\psi(i,j+1)-\psi(i,j-1)}{2W/my} \quad (11)$$

These equations have been utilized for estimating the field dependent mobility and the drain current characteristics. The field dependent mobility has been obtained from

$$\mu_X = \xi_S \xi_r E_X \quad (12)$$

$$\mu_y = \xi_S \xi_r E_y \quad (13)$$

The drain current I_{ds} has been calculated by numerically integrating the charge in the channel region, given by

$$I_{ds} = \frac{Z}{L}\int_0^{V_{ds}} \mu_n(E_x,E_y)Q_n(V)dV \quad (14)$$

The charge in the neutral channel region $Q_n(V)$ has been computed by ,

$$Q_n(V)=q\int_{y_{dg}}^{a} N_d(x,y)dy+q\frac{P_{opt}(1-R_m)(1-R_s)\alpha\tau_L}{h\nu}\int_0^a \exp(-\alpha y)dy \quad (15)$$

where, $\mu_n(E_x,E_y)$ is the field dependent mobility of electrons, $Q_n(V)$ is the charge in the neutral channel region, Z is the device width, E_x and E_y are the electric fields in x (horizontal) and y (vertical) directions respectively, y_{dg} is the variation of depletion depth and function of potential distribution in the channel.
The transconductance g_m has been estimated by

$$g_m\{V_{gs}(i)\}\big|_{V_{ds,const}}=\frac{I_{ds}(i+1,j)-I_{ds}(i-1,j)}{V_{gs}(i+1,j)-V_{gs}(i-1,j)} \quad (16)$$

Drain resistance, r_d and the responsivity of the device have been obtained from

$$r_d\{V_{ds}(i)\}\big|_{V_{gs,const}}=\frac{V_{ds}(i+1,j)-V_{ds}(i-1,j)}{I_{ds}(i+1,j)-I_{ds}(i-1,j)} \quad (17)$$

$$R(\lambda)=\frac{I_{ph}}{P_{opt}} \quad (18)$$

3. Computational techniques

The 2D Gaussian's distribution function is used to find the carrier concentration of the channel assuming the channel is non-uniformly doped. The calculated carrier concentration is verified by calculating the width of depletion layer both at the drain end and source end. The basic 2D Poisson's equation is solved using Liebmann's iteration method to determine the potential distribution through out the channel. The numerically estimated channel potential is used to calculate the electric field intensity in the channel and the electric field at every point is used to calculate the mobility of the carrier. The drain current through the channel is obtained by solving Simson's rule.

4. Results and discussion

Computations have been carried out for the GaAs MESFET photo detector at 300K under dark and illuminated condition. The device parameters considered are 100nm, 80nm, 40nm for length, width and depth respectively. The optical absorption coefficient has been assumed to be 10^6/m at the operating wavelength 1μm.The minority carrier lifetime has been taken to be 1μs. The trap density has been assumed to be distributed non-uniformly in the forbidden energy gap. The impurity profiles $N_d(x,y)$ in ion implanted devices resemble a Gaussian distribution function with the maximum concentration at a Projected range and with a standard deviation.

The variation of depletion layer width with channel length at the source and drain end is shown in Fig. 1 and 2 respectively. The channel width is inversely proportional to the carrier concentration from equation (3) and (4). The depletion layer width increases with increasing gate voltage. The depletion layer width is equal to the channel width and the corresponding voltage is called Pinch-off voltage.

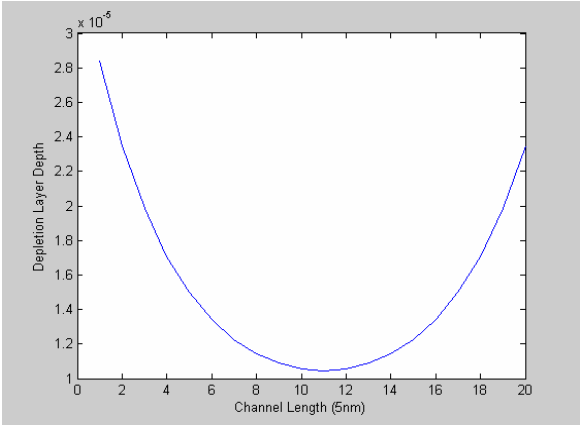

Fig. 1 Variation of the depletion layer width near the source end with respect to channel length.

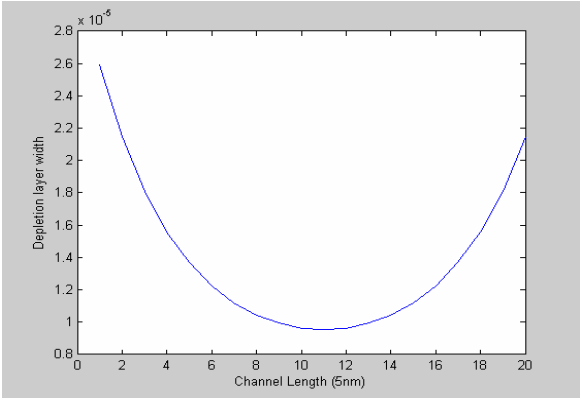

Fig. 2. Variation of the depletion layer width near drain end with respect to channel length.

The potential distribution for dark and illuminated conditions in two dimensional for non-uniformly doped channel is shown in Fig 3. It is found that the potential distribution increases near the source end whereas in the intermediate points are more in the illuminated condition compared to those in the dark condition. The increase in potential is due to the photo generated carriers and the external photovoltaic effects which increases the conductivity of the channel in the illuminated condition.

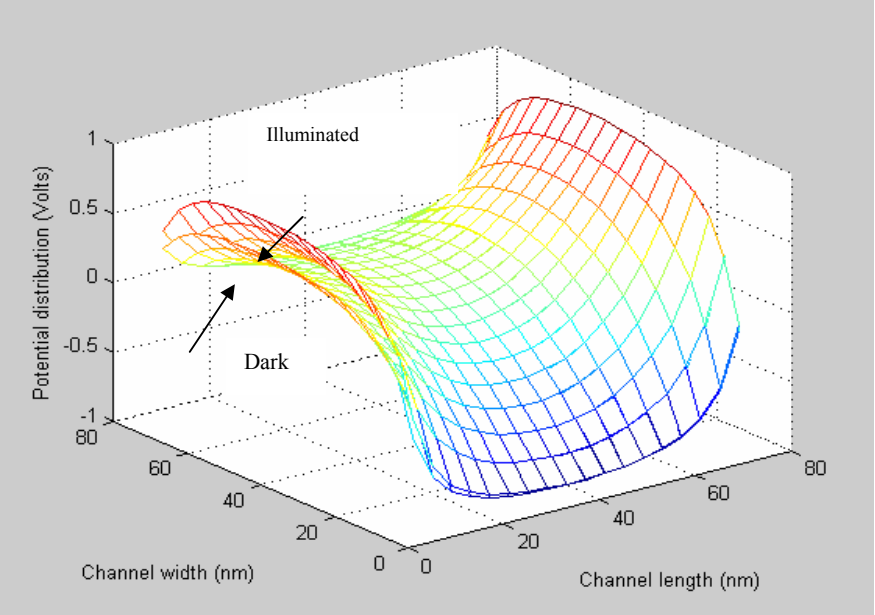

Fig. 3. Variations of Potential Distribution in the Channel under dark and illuminated condition.

The electric field in the x-direction under dark and illuminated condition is shown in Fig. 4. When the device is illuminated, the electric fields along the channel length get decreases because of the reduction in channel resistance. Also it is seen that the electric field along the length of the channel is more dominant than electric field along the width of the device.

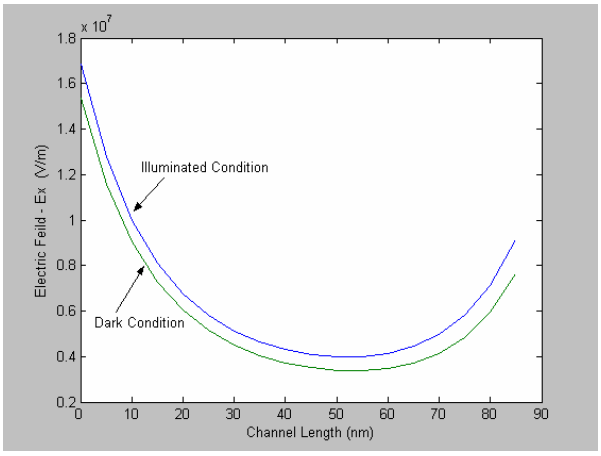

Fig. 4. Electric field variation in the x - direction under dark and illuminated condition.

The electric field in the y-direction under dark and illuminated condition is shown in Fig.5. When the device is illuminated, the electric fields along the channel width of the device also minimized due to reduction in channel resistance.

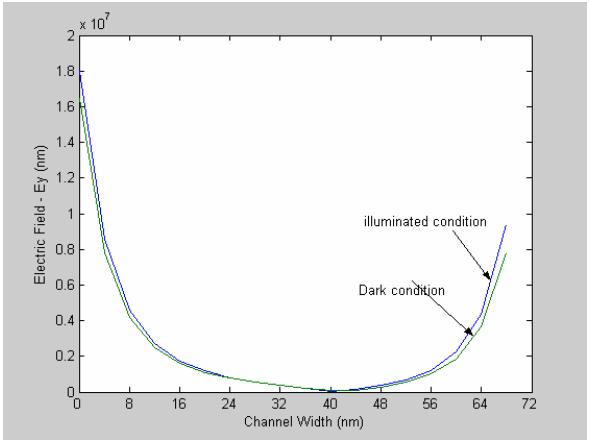

Fig. 5. Electric field in variation the y - direction under dark and illuminated condition.

The variation of drain current with applied drain-to-source voltage V_{ds} is shown in Fig. 6 for various values of gate-to-source voltage V_{gs} for the illuminated and dark condition. The increase in drain current in saturation with V_{ds} is due to channel length modulation. The pinch-off point moves towards the source as V_{ds} increases, effectively shortening the gate length. The electric field becomes stronger in the region between the source and the pinch off point and the carrier velocity is increased. Due to excess carrier generation the drain current of the device get increases under illuminated condition.

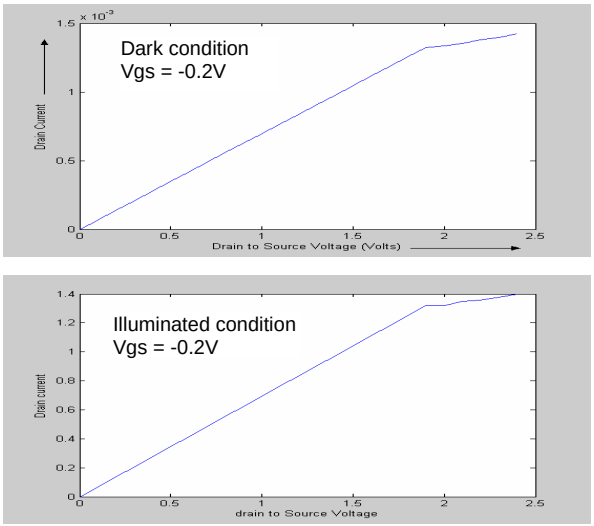

Fig. 6. Variation of the drain current with drain-to-source voltage (V_{ds}) under dark and illuminated conditions.

The transfer characteristics of the GaAs MESFET photodetector is shown in Fig. 7. When the reverse biased gate voltage increases, the resistivity of the channel increases and the drain current get reduced.

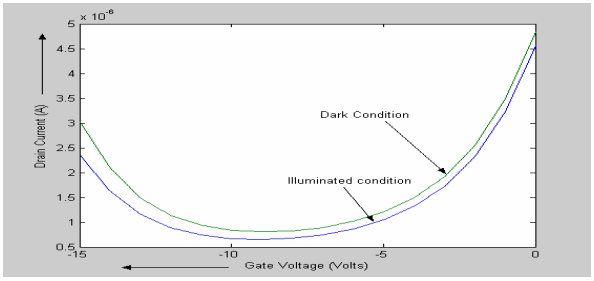

Fig. 7. Transfer characteristics of the MESFET photodetector.

The variation of the transconductenace with the applied gate voltage is depicted in Fig. 8. Transconductance of the device decreases for increase in the gate voltage as it is inversely proportional to the gate voltage.

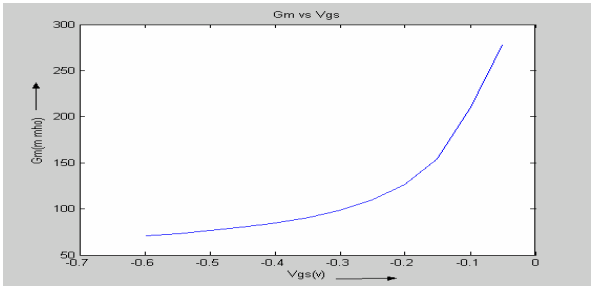

Fig. 8. Variation of the transconductance with applied gate bias.

5. Conclusions

Device characteristics like potential distribution, field distribution and mobility distribution under dark and illuminated condition have been numerically estimated for non-uniformly doped GaAs MESFET. As the device is considered to be non-uniformly doped, it helps us to estimate the real characteristics of the device. Other parameters such as drain characteristics, transfer characteristics, relationship between transconductance and gate voltage are also calculated numerically. It is seen that the device has all qualities to be used as a photo detector in OEIC receivers. The easy realization on GaAs MESFET provides accurate control on the gate length and channel thickness. The present work is confined to modeling and simulation of non-uniformly doped two dimensional GaAs MESFET photodetectors. The future work may be carried out with three dimensional non-uniform doping and also with multi dimensional analysis. The detailed noise analysis can also be carried out to develop an equivalent circuit model for the accurate characteristics of the device for the use in OEIC applications.

References

[1] Prashant Pandey, B. B. Pal, S. Jit, IEEE Trans. Electron Devices **51**, 246 (2004).
[2] R. N. Simons, K. B. Bashin, IEEE Trans. Microwave Theory and Tech., MTT **34**, 1349 (1986).
[3] A. Paolella, A. Madjar, P.R. Herezfeld, IEEE Trans. Microwave Theory and Tech., MTT **42**, 1122 (1994).
[4] J. L. Gautier, D. Pasquet, P. Pouvil, IEEE Trans. Microwave Theory and Tech., MTT **33**, 819 (1985).
[5] J. C. Gammel, J. M. Ballantyne IEEE Int. Electron Dev. Meet. Dig. 120 (1978).
[6] S. M. Sze, "Physics of semiconductor Devices, 2nd Edition, Wiley Eastern Ltd., New Delhi, India, 1981
[7] Madheswaran Muthusamy, Kalaiarasi Kuppusamy, Proceedings of the SPIE, **5881**, 17 (2005).
[8] C. Baack, G. Elze, W. Walf, Electron. Lett. **13**, 193 (1977).
[9] A. Madjar, A. Paolilla, P. R.Herczfeld, IEEE Trans. Microwave Theory Tech., MTT-**40**, 1681 (1992).
[10] P. Chakrabarti, N. L. Shrestha, S. Srivastava, V. Khemka, IEEE Trans. Electron Devices. **39**, 2050(1992).
[11] S. P.Chin, C. Y. Wu, IEEE Trans. Computer Aided Design **11**, 1508 (1992).
[12] J. C. Gammel, J. M. Ballantyne, Appl. Phys. Lett. **36**, 149 (1980).

*Corresponding author: rajamani@rediffmail.com